Eur. Phys. J. C (2021) 81:787
https://doi.org/10.1140/epjc/s10052-021-09571-1

THE EUROPEAN PHYSICAL JOURNAL C

Regular Article -Theoretical Physics

Probing the dark axion portal with muon anomalous magnetic moment

Shao-Feng Ge[1,2,a], **Xiao-Dong Ma**[1,2,b], **Pedro Pasquini**[1,2,c]

[1] Tsung-Dao Lee Institute and School of Physics and Astronomy, Shanghai Jiao Tong University, Shanghai 200240, China
[2] Key Laboratory for Particle Astrophysics and Cosmology (MOE) and Shanghai Key Laboratory for Particle Physics and Cosmology, Shanghai Jiao Tong University, Shanghai 200240, China

Received: 13 May 2021 / Accepted: 23 August 2021 / Published online: 5 September 2021

Abstract We propose a new scenario of using the dark axion portal at one-loop level to explain the recently observed muon anomalous magnetic moment by the Fermilab Muon g-2 experiment. Both axion/axion-like particle (ALP) and dark photon are involved in the same vertex with photon. Although ALP or dark photon alone cannot explain muon $g-2$, since the former provides only negative contribution while the latter has very much constrained parameter space, dark axion portal can save the situation and significantly extend the allowed parameter space. The observed muon anomalous magnetic moment provides a robust probe of the dark axion portal scenario.

1 Introduction

The muon anomalous magnetic moment $a_\mu \equiv (g_\mu - 2)/2$, where g_μ is the muon g-factor, is one of the most precisely measured physical parameters in the Standard Model (SM) of particle physics [1–3]. The Muon g-2 experiment [4,5] at Fermilab provides the currently best measurement [6]

$$a_\mu^{\rm exp}({\rm FNAL}) = 116592040\,(54) \times 10^{-11}, \tag{1}$$

which is consistent with the previous measurement $116592080\,(63) \times 10^{-11}$ [7] by the E821 experiment at Brookhaven National Laboratory (BNL). Then the world average becomes

$$a_\mu^{\rm exp} = 116592061\,(41) \times 10^{-11}. \tag{2}$$

From the BNL result to the Fermilab one, both the central value and the uncertainty decreases.

Huge amount of work has been done to match the unprecedented precision. The SM contribution to a_μ contains four parts [8],

$$a_\mu^{\rm SM} = a_\mu^{\rm QED} + a_\mu^{\rm EW} + a_\mu^{\rm HVP} + a_\mu^{\rm HLbL}. \tag{3}$$

The first two are the QED and electroweak (EW) predictions, respectively, while $a_\mu^{\rm HVP}$ is the hadronic vacuum polarization (HVP) and $a_\mu^{\rm HLbL}$ the hadronic light-by-light (HLbL) contribution. Although the biggest source of uncertainty comes from the hadronic part [9–12], the most recent calculations [13–15] have included the updated measurement of the hadronic contributions [16–18]. The latest theoretical calculation [21] gives

$$a_\mu^{\rm SM} = 116591810\,(43) \times 10^{-11}, \tag{4}$$

where the uncertainty mainly comes from the hadronic vacuum polarization $a_\mu^{\rm HVP}$ and the light-by-light part $a_\mu^{\rm HLbL}$.

The longstanding discrepancy [2,19] between theoretical predictions [20,21] and experimental results is also observed by the new measurement (2) at Fermilab with $4.2\,\sigma$ significance (combined with BNL E821),

$$\Delta a_\mu \equiv a_\mu^{\rm exp} - a_\mu^{\rm SM} = 251\,(59) \times 10^{-11}. \tag{5}$$

The discrepancy increases from $3.7\,\sigma$ to $4.2\,\sigma$ from the BNL measurement to the new world average.

Due to its unprecedented precision, the muon anomalous magnetic moment provides a sensitive probe of new physics (NP) beyond the SM [22–24]. The previous $3.7\,\sigma$ discrepancy between the E821 measurement and the SM prediction has stimulated many novel ideas. An incomplete list includes lepton flavor violation [25], Z' [26–29], neutral scalars [30–33], ALP [34], leptoquarks [35,36], supersymmetry [37–44], dark photon [45–49], and dark matter portals [50–55].

In this letter, we explore the possibility that the dark axion portal [56] with coupling among ALP a, photon γ, and a massive dark photon γ' can explain the observed muon anomalous magnetic moment at the Fermilab Muon g-2 experiment. Since this dimension-5 operator was proposed only recently

[a] e-mail: gesf@sjtu.edu.cn
[b] e-mail: maxid@sjtu.edu.cn (corresponding author)
[c] e-mail: ppasquini@sjtu.edu.cn (corresponding author)

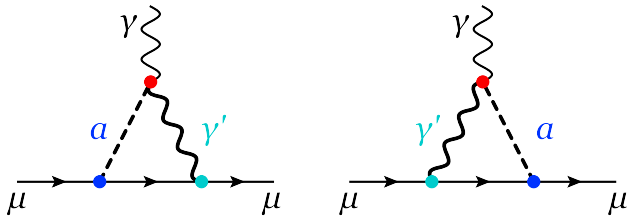

Fig. 1 The one-loop contribution to the muon anomalous magnetic moment from the dark axion portal that couples photon (γ), ALP (a), and dark photon (γ')

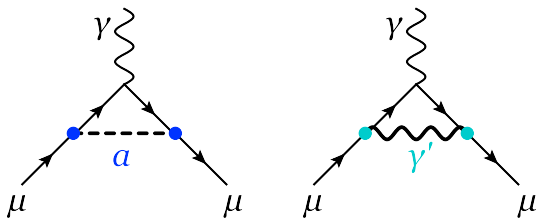

Fig. 2 The ALP (left) and dark photon (right) contributions to the muon anomalous magnetic moment

and involves two invisible particles, its coupling $C_{a\gamma\gamma'}$ is not strongly constrained yet. With TeV scale new physics, $C_{a\gamma\gamma'} \sim 3/\text{TeV}$, a sizable parameter space is still available as we will elaborate in this letter.

2 The dark axion portal contribution

The dark axion portal [56] establishes the connection between the visible sector with the dark one via not just a single ALP or a single photon but both of them,

$$\mathcal{L} \ni \frac{1}{2} C_{a\gamma\gamma'} a F^{\mu\nu} \widetilde{X}_{\mu\nu}, \tag{6}$$

where $F_{\mu\nu} \equiv \partial_\mu A_\nu - \partial_\nu A_\mu$ is the photon field strength. Through this dimension-5 operator, the CP-violating ALP a couples with the dual field strength of dark photon $\widetilde{X}_{\mu\nu} \equiv \frac{1}{2}\epsilon_{\mu\nu\alpha\beta} X^{\alpha\beta}$ where $X_{\mu\nu} \equiv \partial_\mu X_\nu - \partial_\nu X_\mu$. As shown in Fig. 1, the dark axion portal can contribute to the muon anomalous magnetic moment if the ALP and dark photon also couple with muon,

$$\mathcal{L} \ni y_a^\mu a \bar{\mu} (i\gamma_5) \mu - \epsilon e \bar{\mu} \gamma^\nu \mu X_\nu. \tag{7}$$

Here, y_a^μ is the Yukawa coupling with ALP while ϵ is the kinetic mixing between the dark photon and photon, $\frac{1}{2}\epsilon F_{\mu\nu} X^{\mu\nu}$. In principle, the ALP coupling with two photons can also contribute by replacing the dark photon in Fig. 1 with a photon [34,57]. However, due to its stringent constraint, we omit this diagram for simplicity.

The contribution of dark axion portal depicted in Fig. 1 is divergent. With the cut-off regularization, the result can be expressed in terms of the ultra-violet (UV) scale Λ,

$$a_\mu = \frac{m_\mu}{4\pi^2} \epsilon y_a^\mu C_{a\gamma\gamma'} G, \tag{8a}$$

where the loop function G is

$$G \equiv \int_0^1 dx \Bigg[(1-x) \left(\ln \frac{\Lambda^2}{(1-x)m_a^2 + x^2 m_\mu^2} - \frac{1}{2} \right) - \frac{(1-x)m_{\gamma'}^2 + 2x^2 m_\mu^2}{m_a^2 - m_{\gamma'}^2} \ln \frac{(1-x)m_a^2 + x^2 m_\mu^2}{(1-x)m_{\gamma'}^2 + x^2 m_\mu^2} \Bigg], \tag{8b}$$

as a function of the ALP mass m_a, the dark photon mass $m_{\gamma'}$, and the muon mass m_μ. The dark axion portal contribution (8a) has linear dependence on the Yukawa coupling y_a^μ. When y_a^μ is larger than the SM counterpart m_μ/v where $v \approx 246$ GeV is the Higgs vacuum expectation value, the dark axion portal contribution can be enhanced in comparison with the SM one. Similar feature has been observed and named as chiral enhancement in many models but with quadratic dependence [58–60].

Since the interaction in (6) is non-renormalizable, it is only valid up to some cut-off scale $\sim C_{a\gamma\gamma'}^{-1}$. In addition, the divergent loop integral can be assumingly regularized by a similar cut-off Λ with origin from the same UV physics. However, the predicted a_μ in (8a) has mild dependence on Λ which only appears in a log function. Orders of variation in Λ can only change a_μ by several times which can be easily compensated by tuning couplings. For comparison, the Yukawa coupling y_a^μ and the kinetic mixing parameter ϵ are dimensionless, hence cannot directly reflect the new physics scale.

The dark axion portal can also contribute to the muon anomalous magnetic moment at two-loop level via the photon vacuum polarization sub-diagram [61]. However, this contribution is always negative and numerically negligible. For example, with $C_{a\gamma\gamma'} = 3\ \text{TeV}^{-1}$, the two-loop contribution is roughly two orders of magnitude smaller than its one-loop counterpart. Therefore, we neglect their contribution and focus on the one-loop diagrams in this letter. Note that the dark axion portal coupling, $C_{a\gamma\gamma'} = 3\ \text{TeV}^{-1}$, adopted here satisfies existing experimental constraints [61].

In principle, the ALP can also couple with the SM Z boson, $\frac{1}{2} C_{a\gamma Z} a F_{\mu\nu} \tilde{Z}^{\mu\nu}$ [62,63]. Then a similar contribution from the ALP-photon-Z vertex, by replacing the dark photon γ' in Fig. 1 with Z. The analytical formula (8) still applies after replacing the dark photon mass $m_{\gamma'}$ by the Z boson mass m_Z, the coupling constants $C_{a\gamma\gamma'}$ by $C_{a\gamma Z}$ and $e\epsilon$ by $g_V = \frac{g}{c_W}\left(\frac{1}{4} - s_W^2\right) \approx 4.5 \times 10^{-2} e$ of the vector part of the Z-muon coupling while the axial-vector part does not contribute due to the mismatch of parity and charge conjugation properties. The good thing is that the Z coupling with muon and the Z boson mass have already been measured, hence reducing the number of parameters by two. However, the current bound

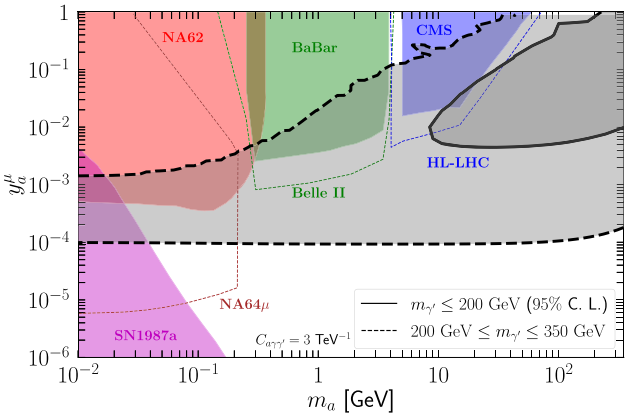

Fig. 3 Experimental constraints on the ALP Yukawa coupling with muon from (1) supernova cooling from SN1987a (purple region) [69]; (2) kaon decay $K \to \mu\nu a$ [66] (red region) at NA62; (3) final-state radiation $e^+e^- \to \mu^+\mu^- a$ (green region) at the BaBar experiment [66,70]; (4) rare Z decay (blue region) at CMS [71]. The projected sensitivities at NA64 (brown dashed line) [67], Belle II (green dashed line), and HL-LHC (blue dashed line) [68] are also shown for comparison. The black contours are the allowed region for explaining the observed muon anomalous magnetic moment together with dark axion portal at 95% CL

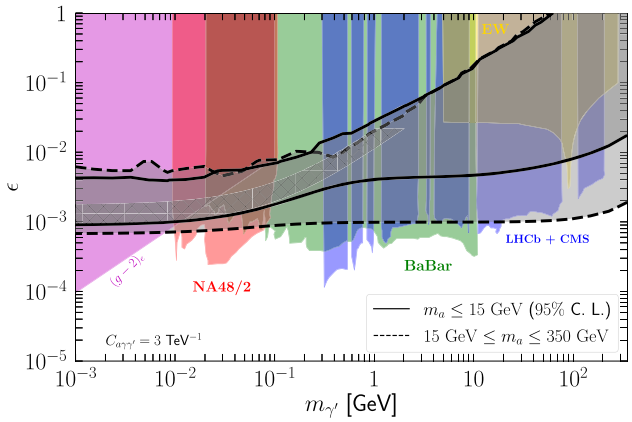

Fig. 4 Experimental constraints on the dark photon kinetic mixing parameter ϵ as a function of the dark photon mass $m_{\gamma'}$ from: (1) electron anomalous magnetic moment $(g-2)_e$ (purple) [46]; (2) resonant production of dark photon at the BaBar experiment (green) [73]; (3) dark photon from pion decay at the NA48 experiment (red) [74]; (4) dark photon production from various mesons at LHCb [75,76] and Higgs at CMS (blue) [77]; (5) electroweak precision observables (yellow) [78]. The hashed band is the allowed region for explaining the muon g-2 with dark photon alone while the black contour is obtained together with dark axion portal at 95% CL

on the coupling $C_{a\gamma Z} \lesssim 0.03$ TeV^{-1} [64] from the anomalous Z decay $Z \to \gamma a$ [65] is rather stringent. The contribution from the ALP-photon-Z vertex is negligibly small.

3 The individual contribution of ALP or dark photon

The ALP or dark photon alone can also contribute to the muon anomalous magnetic moment as shown in Fig. 2. We first consider the contribution from the ALP which is finite,

$$a_\mu^a = \frac{(y_a^\mu)^2}{4\pi^2}\frac{m_\mu^2}{m_a^2}F_a\left(\frac{m_\mu}{m_a}\right), \tag{9a}$$

$$F_a(\eta) \equiv -\frac{1}{2}\int_0^1 \mathrm{d}x \frac{x^3}{(1-x)\left(1-\eta^2 x\right)+\eta^2 x}. \tag{9b}$$

Note that this ALP-only contribution is negative [34] since $F_a(\eta) \lesssim 0$ where $\eta \equiv m_\mu/m_a$. The pseudoscalar case is completely different from the scalar scenario which can contribute a positive term. A pseudoscalar alone cannot explain why the observed $a_\mu^{\rm exp}$ is larger than the SM prediction $a_\mu^{\rm SM}$ unless the experimental measurement is smaller than the theoretical prediction.

The contribution from the dark photon shown in the right panel of Fig. 2 takes the form as [45–47],

$$a_\mu^{\gamma'} = \frac{\epsilon^2 e^2}{4\pi^2}\frac{m_\mu^2}{m_{\gamma'}^2}F_{\gamma'}\left(\frac{m_\mu}{m_{\gamma'}}\right), \tag{10a}$$

$$F_{\gamma'}(\eta) \equiv \frac{1}{2}\int_0^1 \mathrm{d}x \frac{2x^2(1-x)}{(1-x)\left(1-\eta^2 x\right)+\eta^2 x}, \tag{10b}$$

with $\eta \equiv m_\mu/m_{\gamma'}$. Different from the loop function F_a for the ALP-only contribution, $F_{\gamma'} \gtrsim 0$ always holds. It seems that the single contribution from the dark photon can explain the observed muon anomalous magnetic moment. However, the required parameter space in the $m_{\gamma'} - \epsilon$ plane to explain the observed Δa_μ has already been excluded by other experimental bounds [49] as we will discuss in detail below.

4 Parameter space

It is instructive to compare the three distinct contributions: (8a) for dark axion portal, (9) for ALP, and (10) for dark photon,

$$\frac{a_\mu}{a_\mu^a} \sim \frac{\epsilon}{y_a^\mu}\frac{m_a^2 C_{a\gamma\gamma'}}{m_\mu} \sim \frac{\epsilon}{10^{-3}}\frac{0.1}{y_a^\mu}\left(\frac{m_a}{100\ \mathrm{GeV}}\right)^2, \tag{11a}$$

$$\frac{a_\mu}{a_\mu^{\gamma'}} \sim \frac{y_a^\mu}{\epsilon e^2}\frac{m_{\gamma'}^2 C_{a\gamma\gamma'}}{m_\mu} \sim 10^5\frac{10^{-3}}{\epsilon}\frac{y_a^\mu}{0.1}\left(\frac{m_{\gamma'}}{100\ \mathrm{GeV}}\right)^2, \tag{11b}$$

where $C_{a\gamma\gamma'} \sim$ TeV^{-1}. The loop function ratios, G/F_a and $G/F_{\gamma'}$, are dropped out since they are comparable with each other. For the dark axion portal contribution to dominate, $a_\mu \gg a_\mu^a, a_\mu^{\gamma'}$, the ALP and dark photon masses are bounded from below, $m_a \gg \sqrt{y_a^\mu/\epsilon}\,10$ GeV and $m_{\gamma'} \gg \sqrt{\epsilon/y_a^\mu}\,\sqrt{10}$ GeV. If the two dimensionless couplings are comparable with each other, $\epsilon \sim y_a^\mu$, both the ALP mass m_a and the dark photon mass $m_{\gamma'}$ are around the GeV scale.

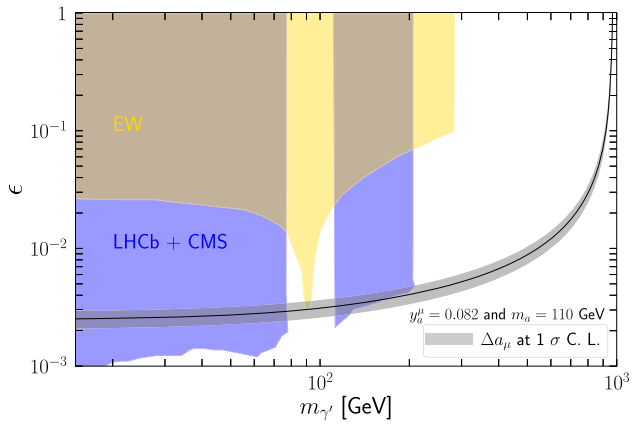

Fig. 5 The allowed region for explaining the muon $g-2$ with the fixed ALP parameters $y_a^\mu = 0.082$ and $m_a = 110$ GeV at 1 σ CL

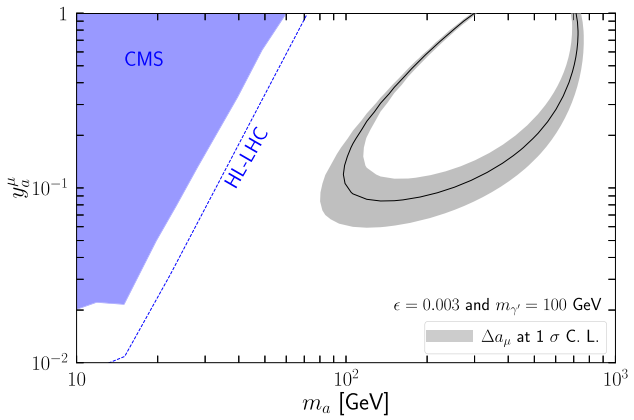

Fig. 6 The allowed ALP region for explaining the muon $g-2$ with the fixed dark photon parameters $\epsilon = 0.003$ and $m_{\gamma'} = 100$ GeV at 1 σ CL

Richer mass patterns can be realized by tuning the two couplings to change the mass limits, or allowing the ALP-only and dark photon-only contributions in Fig. 2 to be comparable with the dark axion portal one in Fig. 1. Below we explore the allowed parameter spaces in detail.

As argued above, the interesting ALP mass is around GeV to a few hundreds of GeV scale. In this range, the experimental constraints [66–68] mainly come from SN1987a, beam dump experiment NA62, low energy electron positron colliders such as BaBar, and collider searches at LHC. We summarize in Fig. 3 those constraints that can apply to the configuration in this letter, where the ALP only couples with muon rather than electron or tau.

The purple region at the left-bottom corner of Fig. 3 is excluded by the supernova (SN) cooling rate from the SN1987a observation [69]. The bound reaches $y_a^\mu \approx 10^{-6}$ and can exclude the mass region up to 0.2 GeV.

The red region in Fig. 3 is excluded by the NA62 experiment [66] using the search of rare kaon decay channel $K \to \mu\nu a$. The probe of m_a is limited by the kaon mass (~ 494 MeV), explaining why the excluded region can only extend to $\lesssim 400$ MeV. For comparison, we also show the projected sensitivity from the $\mu^+ N \to \mu^+ N + a$ process at the NA64 muon beam dump experiment (brown dashed line) [67].

The green region in Fig. 3 was obtained from the BaBar experiment with final-state radiation of the invisible Z' which further decays into a $\mu^+\mu^-$ pair, $e^+e^- \to \mu^-\mu^+ Z' \to \mu^-\mu^+\mu^-\mu^+$. Although this bound is not originally obtained for ALP, it can be easily converted [66,70]. The BaBar experiment is an electron-positron collider with center-of-mass energy around 10 GeV. Consequently, the sensitive mass region is $m_a \in [0.1, 4]$ GeV. The similar situation happens for the CMS rare Z decay constraint [71] shown as the blue region in Fig. 3 which covers the range from 5 GeV up to 50 GeV. For comparison, we also show the projected sensitivities at Belle II (green dashed line) and HL-LHC [68] (blue dashed line).

It is evident that there is a very large region of the parameter space to be explored for masses above 0.2 GeV. All other constraints compiled in [66–68] involves Yukawa couplings with either electron or tau leptons and hence cannot apply to the configuration considered in this letter. The gap between the BaBar and CMS region can be covered by the future HL-LHC searches (blue dashed line) and Belle II can also increase the sensitivity below 4 GeV (green dashed lines) [68]. Even so, the available parameter space is still quite sizable.

The current bounds [49,72] on the dark photon mass $m_{\gamma'}$ and its kinetic mixing ϵ with photon has been summarized in Fig. 4. These constraints covers the dark photon mass range from 1 MeV to 1 TeV. In contrast to the ALP case, since the kinetic mixing leads to universal coupling between the dark photon and all charged leptons, those experimental constraints involving electron can also apply here. It is interesting to see that the electron anomalous magnetic moment, $(g-2)_e$, excludes the very light dark photon scenario (purple region) [46]. The dark photon can be resonantly produced at the BaBar experiment. With 10 GeV center-of-mass energy, the excluded region (green) spans from around 20 MeV up to roughly 10 GeV [73]. In between, the NA48 searches for dark photon from pion decay cover the red region from 9 to 100 MeV [74]. The decays of various mesons at LHCb [75,76] and Higgs at CMS [77] also give strong constraints shown as gaped blue regions. At CMS, the dark photon is produced from Higgs decay, $h \to Z\gamma'$ and $h \to \gamma'\gamma'$, and it further decays to a pair of muons. The yellow region comes from the electroweak (EW) precision observables [78]. It is interesting to observe that the EW precision observables fill the gap around Z boson mass.

5 Revival with dark axion portal

With the available parameter space compiled in Fig. 3 for ALP and Fig. 4 for dark photon, we are ready to explore the allowed region for explaining the recently observed muon anomalous magnetic moment at Fermilab. This can be quantitatively done with χ^2 function,

$$\chi^2 \equiv \left(\frac{\Delta a_\mu - \Delta a_\mu^{\rm NP}}{\sigma(\Delta a_\mu)} \right)^2 , \tag{12}$$

with central value Δa_μ and uncertainty $\sigma(\Delta a_\mu)$ taken from (5). The new physics prediction $\Delta a_\mu^{\rm NP}$ here contains the four parameters, m_a and y_a^μ for ALP as well as $m_{\gamma'}$ and ϵ for dark photon, in addition to the fixed coupling $C_{a\gamma\gamma'} = 3$ TeV^{-1} and cut-off $\Lambda = 1$ TeV. To illustrate the allowed parameter space of ALP, for each point of Fig. 3 the values of m_a and y_a^μ are fixed while the dark photon parameters $m_{\gamma'}$ and ϵ are varied to obtain the smallest value $\chi^2_{\rm min}(m_a, y_a^\mu)$. The dark photon parameters scan in the range $m_{\gamma'} \in [10^{-3}, 350]$ GeV and $\epsilon \in [10^{-5}, 1]$. However, those points that fall inside the experimentally excluded regions of Fig. 4 are not included in the scan. The resulting $\chi^2_{\rm min}(m_a, y_a^\mu)$ is then a marginalized χ^2 function of just the two ALP parameters. Similar procedures can also produce a marginalized $\chi^2_{\rm min}(m_{\gamma'}, \epsilon)$ after scanning the ALP parameters in the range of $m_a \in [10^{-2}, 350]$ GeV and $y_a^\mu \in [10^{-6}, 1]$ but deducting experimentally excluded regions. So from Fig. 3 we can read off the values of m_a and y_a^μ, but not the corresponding values of $m_{\gamma'}$ and ϵ. The similar situation happens for Fig. 4. The black contours of m_a and y_a^μ in Fig. 3 are obtained with $\chi^2_{\rm min}(m_a, y_a^\mu) < 5.99$ at 95% CL and similarly for Fig. 4.

The black contours in Fig. 3 cover a large part of the remaining parameter space. As argued at the beginning of this section, the ALP mass is bounded from below, $m_a \gg \sqrt{y_a^\mu/\epsilon}\, 10$ GeV, in order for the dark axion portal contribution to dominate. With smaller Yukawa coupling y_a^μ, the ALP mass can also be smaller and hence cover the whole mass range in Fig. 3. The ALP contribution is always negative [34] no matter what is the sign of the Yukawa coupling y_a^μ as indicated by (9). This forbids the possibility of using only ALP to explain the observed positive Δa_μ. However, in the presence of dark axion portal, the ALP or pseudoscalar at large receives significant parameter space to explain the muon anomalous magnetic moment. Although the black contour is marginalized over the dark photon parameters, namely its mass $m_{\gamma'}$ and kinetic mixing ϵ, we can still show the dependence on the dark photon mass by specifying the mass range of dark photon to be marginalized over. The solid black contour is obtained with $m_{\gamma'} \leq 200$ GeV while the dashed one with 200 GeV $\leq m_{\gamma'} \leq 350$ GeV. It is interesting to see that with larger dark photon mass, the allowed ALP parameter space becomes larger with the Yukawa coupling y_a^μ touching down to as small as 10^{-4}. The ALP solution can be readily saved by the dark axion portal.

For the dark photon parameter space illustrated in Fig. 4, almost all mass range below 200 GeV has been experimentally constrained to $\epsilon \lesssim 10^{-3}$. Especially, the required parameter space, the hashed region in Fig. 4, for dark photon to explain the muon anomalous magnetic moment has been excluded by various observations including electron $(g-2)_e$, NA48/2, BaBar, and LHCb+CMS. It is very interesting to see that the dark axion portal coupling can also help to save the situation. Now the required parameter space significantly expands to the black contours, the solid one for $m_a \leq 15$ GeV and the dashed one for 15 GeV $\leq m_a \leq 350$ GeV. The heavy mass region, $m_{\gamma'} \gtrsim \mathcal{O}(10)$ GeV, still has sizable space. Even the low mass region around $m_{\gamma'} \approx 10$ MeV opens for 15 GeV $\leq m_a \leq 350$ GeV.

In the large mass limit ($m_a, m_{\gamma'} \gg m_\mu$), the total contribution shows decoupling features. To make it explicit, we fix the ALP parameters, $m_a = 110$ GeV and $y_a^\mu = 0.082$, as an example. The total contribution $\Delta a_\mu(m_{\gamma'}, \epsilon)$ is then a function of the two dark photon parameters $m_{\gamma'}$ and ϵ. Fig. 5 shows the allowed region of $\Delta a_\mu(m_{\gamma'}, \epsilon) = (251 \pm 59) \times 10^{-11}$ as grey area. With larger dark photon mass, the dark photon coupling ϵ also needs to increase to maintain the prediction of $\Delta a_\mu(m_{\gamma'}, \epsilon)$. Otherwise, for a fixed ϵ, the predicted $\Delta a_\mu(m_{\gamma'}, \epsilon)$ would decrease with the dark photon mass. This decoupling behavior can be understood analytically with the approximate forms of (8)–(10) in the large mass limit,

$$a_\mu \approx \frac{m_\mu}{4\pi^2} \epsilon y_a^\mu C_{a\gamma\gamma'} \frac{m_a^2 \ln \frac{\Lambda}{m_a} - m_{\gamma'}^2 \ln \frac{\Lambda}{m_{\gamma'}}}{m_a^2 - m_{\gamma'}^2}, \tag{13a}$$

$$a_\mu^a \approx -\left(\frac{y_a^\mu}{2\pi}\right)^2 \frac{m_\mu^2}{m_a^2} \left(\ln \frac{m_a}{m_\mu} - \frac{11}{12} \right), \tag{13b}$$

$$a_\mu^{\gamma'} \approx \frac{1}{3} \left(\frac{\epsilon e}{2\pi}\right)^2 \frac{m_\mu^2}{m_{\gamma'}^2}. \tag{13c}$$

For $m_{\gamma'} \gg m_a$, we can see that $a_\mu \propto \ln \frac{\Lambda}{m_{\gamma'}}$ and $a_\mu^{\gamma'} \propto 1/m_{\gamma'}^2$. Both terms decrease with $m_{\gamma'}$ and hence have decoupling behavior.

Figure 6 shows the decoupling behavior in the ALP parameter space. Taking the two dark photon parameters, $m_{\gamma'} = 100$ GeV and $\epsilon = 0.003$, the allowed region of $\Delta a_\mu(m_a, y_a^\mu) = (251 \pm 59) \times 10^{-11}$ in the $m_a - y_a^\mu$ plane is the grey area. Since $y_a^\mu \sim \mathcal{O}(10^{-1})$ is relatively large, both a_μ^a and a_μ provide the dominant contributions, one has quadratic dependence on y_a^μ and the other linear. Consequently, for a given ALP mass m_a, there are two possible solutions for the Yukawa coupling y_a^μ to match the experimental result. This is why the grey area of Fig. 6 is a circle rather than a line as in Fig. 5.

For $m_a \gg m_{\gamma'}$, we can also see decoupling features: with larger ALP mass the prediction $\Delta a_\mu(m_a, y_a^\mu)$ becomes smaller. This is because both $a_\mu \propto \ln \frac{\Lambda}{m_a}$ and $a_\mu^a \approx (m_\mu^2/m_a^2)\ln(m_a/m_\mu)$ decrease with m_a. With larger ALP mass, the Yukawa coupling y_a^μ should also increase in order to maintain the same prediction of $\Delta a_\mu(m_a, y_a^\mu)$.

However, with both dark photon and ALP parameters, the decoupling features are not transparent. For illustration, we take $m_{\gamma'} = 100$ GeV, $m_a = 110$ GeV, and $\epsilon = 3 \times 10^{-3}$ (combined with our assumptions: $C_{a\gamma\gamma'} = 3$ TeV^{-1} and $\Lambda = 1$ TeV), leading to,

$$a_\mu \approx 4.2 \times 10^{-8} y_a^\mu, \quad a_\mu^a \approx -1.4 \times 10^{-7} (y_a^\mu)^2, \tag{14}$$

together with $a_\mu^{\gamma'} \ll \Delta a_\mu$. Then either $y_a^\mu = 0.082$ or $y_a^\mu = 0.22$ gives the observed discrepancy. The points $(m_a, y_a^\mu) = (110\ \text{GeV}, 0.082 \text{ or } 0.22)$ and $(m_{\gamma'}, \epsilon) = (100\ \text{GeV}, 3 \times 10^{-3})$ are inside our 95% CL band in Figs. 3 and 4, as expected, but y_a^μ and ϵ need not to be of the same order. In other words, the presence of both contributions can in fact enlarge the parameter space, including larger values of m_a and $m_{\gamma'}$.

6 Conclusion

The latest measurement of the muon anomalous magnetic moment at the Fermilab Muon g-2 experiment further enhances the discrepancy with theoretical prediction from 3.7σ to 4.2σ. This clearly indicates that there is something new beyond the SM, although a decisive conclusion still awaits more data. On one hand, this discrepancy enhances theoretical exploration of possible solutions. But on the other, some solutions have been already excluded, including either the ALP or dark photon scenario. Even though the dark axion portal was originally motivated as a way to connect the visible world with the dark side, it can surprisingly save the ALP and dark photon for explaining the muon anomalous magnetic moment. Since dark matter contributes five times more energy density in the Universe than the ordinary matter and the latter already has rich particle spectrum, there is no reason to assume that the dark sector is composed of a single particle. In this sense, the dark axion portal provides a more interesting option than just ALP or dark photon. And muon anomalous magnetic moment can provide a robust probe of this new scenario.

Acknowledgements This work is supported by the Double First Class start-up fund (WF220442604), the Shanghai Pujiang Program (20PJ1407800), and National Natural Science Foundation of China (No. 12090064). This work is also supported in part by Chinese Academy of Sciences Center for Excellence in Particle Physics (CCEPP).

Data Availability Statement This manuscript has no associated data or the data will not be deposited. [Authors' comment: Our work is theoretical/phenomenological. We did not generate new data. We analyzed the data from the $g-2$ experiment cited in reference [6]. The codes we used for the plots can be provided upon request.]

Funded by SCOAP[3].

References

1. J.P. Miller, E. de Rafael, B.L. Roberts, D. Stöckinger, Muon (g-2): experiment and theory. Ann. Rev. Nucl. Part. Sci. **62**, 237–264 (2012). https://doi.org/10.1146/annurev-nucl-031312-120340
2. F. Jegerlehner, The anomalous magnetic moment of the muon. Springer Tracts Mod. Phys. **274**, 1–693 (2017). https://doi.org/10.1007/978-3-319-63577-4
3. P.A. Zyla et al. (Particle Data Group), Review of particle physics. PTEP **2020**(8), 083C01 (2020). https://doi.org/10.1093/ptep/ptaa104
4. J. Grange et al. (Muon g-2), Muon (g-2) technical design report. arXiv:1501.06858 [physics.ins-det]
5. A. Keshavarzi (Muon g-2), The muon $g-2$ experiment at Fermilab. EPJ Web Conf. **212**, 05003 (2019). https://doi.org/10.1051/epjconf/201921205003. arXiv:1905.00497 [hep-ex]
6. B. Abi et al. (Muon g-2 Collaboration), Measurement of the positive muon anomalous magnetic moment to 0.46 ppm. Phys. Rev. Lett. **126**, 141801 (2021). https://doi.org/10.1103/PhysRevLett.126.141801. arXiv:2104.03281 [hep-ex]
7. G.W. Bennett et al. (Muon g-2), Final report of the muon E821 anomalous magnetic moment measurement at BNL. Phys. Rev. D **73**, 072003 (2006). https://doi.org/10.1103/PhysRevD.73.072003. arXiv:hep-ex/0602035
8. A. Keshavarzi, D. Nomura, T. Teubner, $g-2$ of charged leptons, $\alpha(M_Z^2)$, and the hyperfine splitting of muonium. Phys. Rev. D **101**(1), 014029 (2020). https://doi.org/10.1103/PhysRevD.101.014029. arXiv:1911.00367 [hep-ph]
9. K. Hagiwara, A.D. Martin, D. Nomura, T. Teubner, Predictions for g-2 of the muon and alpha(QED) (M**2(Z)). Phys. Rev. D **69**, 093003 (2004). https://doi.org/10.1103/PhysRevD.69.093003. arXiv:hep-ph/0312250
10. A. Gérardin, The anomalous magnetic moment of the muon: status of Lattice QCD calculations. Eur. Phys. J. A **57**(4), 116 (2021). https://doi.org/10.1140/epja/s10050-0-1-00426-7. arXiv:2012.03931 [hep-lat]
11. E.H. Chao, R.J. Hudspith, A. Gérardin, J.R. Green, H.B. Meyer, K. Ottnad, Hadronic light-by-light contribution to $(g-2)_\mu$ from lattice QCD: a complete calculation. Eur. Phys. J. C **81**(7), 651 (2021). https://doi.org/10.1140/epjc/s10052-021-09455-4. arXiv:2104.02632 [hep-lat]
12. S. Borsanyi, Z. Fodor, J.N. Guenther, C. Hoelbling, S.D. Katz, L. Lellouch, T. Lippert, K. Miura, L. Parato, K.K. Szabo et al., Leading hadronic contribution to the muon 2 magnetic moment

from lattice QCD. Nature **593**, 51–55 (2021). https://doi.org/10.1038/s41586-021-03418-1. arXiv:2002.12347 [hep-lat]
13. T. Blum et al. (RBC and UKQCD), Calculation of the hadronic vacuum polarization contribution to the muon anomalous magnetic moment. Phys. Rev. Lett. **121**(2), 022003 (2018). https://doi.org/10.1103/PhysRevLett.121.022003. arXiv:1801.07224 [hep-lat]
14. T. Blum, N. Christ, M. Hayakawa, T. Izubuchi, L. Jin, C. Jung, C. Lehner, Hadronic light-by-light scattering contribution to the muon anomalous magnetic moment from lattice QCD. Phys. Rev. Lett. **124**(13), 132002 (2020). https://doi.org/10.1103/PhysRevLett.124.132002. arXiv:1911.08123 [hep-lat]
15. M. Davier, A. Hoecker, B. Malaescu, Z. Zhang, A new evaluation of the hadronic vacuum polarisation contributions to the muon anomalous magnetic moment and to $\alpha(m_Z^2)$. Phys. Rev. D **101**(1), 014029 (2020). https://doi.org/10.1140/epjc/s10052-020-7792-2. arXiv:1908.00921 [hep-ph] [Erratum: Eur. Phys. J. C **80**(5), 410 (2020)]
16. T. Xiao, S. Dobbs, A. Tomaradze, K.K. Seth, G. Bonvicini, Precision measurement of the hadronic contribution to the muon anomalous magnetic moment. Phys. Rev. D **97**(3), 032012 (2018). https://doi.org/10.1103/PhysRevD.97.032012. arXiv:1712.04530 [hep-ex]
17. J.P. Lees et al. (BaBar), Study of the reactions $e^+e^- \to \pi^+\pi^-\pi^0\pi^0\pi^0\gamma$ and $\pi^+\pi^-\pi^0\pi^0\eta\gamma$ at center-of-mass energies from threshold to 4.35 GeV using initial-state radiation. Phys. Rev. D **98**(11), 112015 (2018). https://doi.org/10.1103/PhysRevD.98.112015. arXiv:1907.01556 [hep-ex]
18. M. Hoferichter, B.L. Hoid, B. Kubis, Three-pion contribution to hadronic vacuum polarization. JHEP **08**, 137 (2019). https://doi.org/10.1007/JHEP08(2019)137. arXiv:1907.01556 [hep-ph]
19. M. Benayoun, P. David, L. DelBuono, F. Jegerlehner, Muon $g-2$ estimates: can one trust effective Lagrangians and global fits? Eur. Phys. J. C **75**(12), 613 (2015). https://doi.org/10.1140/epjc/s10052-015-3830-x. arXiv:1507.02943 [hep-ph]
20. F. Jegerlehner, A. Nyffeler, The muon $g-2$. Phys. Rep. **477**, 1–110 (2009). https://doi.org/10.1016/j.physrep.2009.04.003. arXiv:0902.3360 [hep-ph]
21. T. Aoyama et al., The anomalous magnetic moment of the muon in the Standard Model. Phys. Rep. **887**, 1–166 (2020). https://doi.org/10.1016/j.physrep.2020.07.006. arXiv:2006.04822 [hep-ph]
22. A. Czarnecki, W.J. Marciano, The muon anomalous magnetic moment: a harbinger for 'new physics'. Phys. Rev. D **64**, 013014 (2001). https://doi.org/10.1103/PhysRevD.64.013014. arXiv:hep-ph/0102122
23. W. Yin, M. Yamaguchi, Muon $g-2$ at multi-TeV muon collider. arXiv:2012.03928 [hep-ph]
24. R. Capdevilla, D. Curtin, Y. Kahn, G. Krnjaic, A no-lose theorem for discovering the new physics of $(g-2)_\mu$ at muon colliders. arXiv:2101.10334 [hep-ph]
25. M. Lindner, M. Platscher, F.S. Queiroz, A call for new physics: the muon anomalous magnetic moment and lepton flavor violation. Phys. Rep. **731**, 1–82 (2018). https://doi.org/10.1016/j.physrep.2017.12.001. arXiv:1610.06587 [hep-ph]
26. S.N. Gninenko, N.V. Krasnikov, The muon anomalous magnetic moment and a new light gauge boson. Phys. Lett. B **513**, 119 (2001). https://doi.org/10.1016/S0370-2693(01)00693-1. arXiv:hep-ph/0102222
27. S. Baek, N.G. Deshpande, X.G. He, P. Ko, Muon anomalous g-2 and gauged L(muon) - L(tau) models. Phys. Rev. D **64**, 055006 (2001). https://doi.org/10.1103/PhysRevD.64.055006. arXiv:hep-ph/0104141
28. E. Ma, D.P. Roy, S. Roy, Gauged L(mu)–L(tau) with large muon anomalous magnetic moment and the bimaximal mixing of neutrinos. Phys. Lett. B **525**, 101–106 (2002). https://doi.org/10.1016/S0370-2693(01)01428-9. arXiv:hep-ph/0110146
29. W. Altmannshofer, C.Y. Chen, P.S. Bhupal Dev, A. Soni, Lepton flavor violating Z' explanation of the muon anomalous magnetic moment. Phys. Lett. B **762**, 389–398 (2016). https://doi.org/10.1016/j.physletb.2016.09.046. arXiv:1607.06832 [hep-ph]
30. A. Crivellin, J. Girrbach, U. Nierste, Yukawa coupling and anomalous magnetic moment of the muon: an update for the LHC era. Phys. Rev. D **83**, 055009 (2011). https://doi.org/10.1103/PhysRevD.83.055009. arXiv:1010.4485 [hep-ph]
31. C.Y. Chen, H. Davoudiasl, W.J. Marciano, C. Zhang, Implications of a light dark Higgs solution to the g_μ-2 discrepancy. Phys. Rev. D **93**(3), 035006 (2016). https://doi.org/10.1103/PhysRevD.93.035006. arXiv:1511.04715 [hep-ph]
32. F. Abu-Ajamieh, Probing scalar and pseudoscalar solutions of the g-2 anomaly. Adv. High Energy Phys. **2020**, 1751534 (2020). https://doi.org/10.1155/2020/175153. arXiv:1810.08891 [hep-ph]
33. S. Jana, P.K. Vishnu, S. Saad, Resolving electron and muon $g-2$ within the 2HDM. Phys. Rev. D **101**(11), 115037 (2020). https://doi.org/10.1103/PhysRevD.101.115037. arXiv:2003.03386 [hep-ph]
34. W.J. Marciano, A. Masiero, P. Paradisi, M. Passera, Contributions of axionlike particles to lepton dipole moments. Phys. Rev. D **94**(11), 115033 (2016). https://doi.org/10.1103/PhysRevD.94.115033. arXiv:1607.01022 [hep-ph]
35. D. Chakraverty, D. Choudhury, A. Datta, A nonsupersymmetric resolution of the anomalous muon magnetic moment. Phys. Lett. B **506**, 103–108 (2001). https://doi.org/10.1016/S0370-2693(01)00419-1. arXiv:hep-ph/0102180
36. K.M. Cheung, Muon anomalous magnetic moment and leptoquark solutions. Phys. Rev. D **64**, 033001 (2001). https://doi.org/10.1103/PhysRevD.64.033001. arXiv:hep-ph/0102238
37. J.A. Grifols, A. Mendez, Constraints on supersymmetric particle masses from $(g-2)\,\mu$. Phys. Rev. D **26**, 1809 (1982). https://doi.org/10.1103/PhysRevD.26.1809
38. R. Barbieri, L. Maiani, The muon anomalous magnetic moment in broken supersymmetric theories. Phys. Lett. B **117**, 203–207 (1982). https://doi.org/10.1016/0370-2693(82)90547-0
39. S.P. Martin, J.D. Wells, Muon anomalous magnetic dipole moment in supersymmetric theories. Phys. Rev. D **64**, 035003 (2001). https://doi.org/10.1103/PhysRevD.64.035003. arXiv:hep-ph/0103067
40. D. Stockinger, The muon magnetic moment and supersymmetry. J. Phys. G **34**, R45–R92 (2007). https://doi.org/10.1088/0954-3899/34/2/R01. arXiv:hep-ph/0609168
41. B.P. Padley, K. Sinha, K. Wang, Natural supersymmetry, muon $g-2$, and the last crevices for the top squark. Phys. Rev. D **92**(5), 055025 (2015). https://doi.org/10.1103/PhysRevD.92.055025. arXiv:1505.05877 [hep-ph]
42. A.S. Belyaev, J.E. Camargo-Molina, S.F. King, D.J. Miller, A.P. Morais, P.B. Schaefers, A to Z of the muon anomalous magnetic moment in the MSSM with Pati-Salam at the GUT scale. JHEP **06**, 142 (2016). https://doi.org/10.1007/JHEP06(2016)142. arXiv:1605.02072 [hep-ph]
43. M. Endo, W. Yin, Explaining electron and muon $g-2$ anomaly in SUSY without lepton-flavor mixings. JHEP **08**, 122 (2019). https://doi.org/10.1007/JHEP08(2019)122. arXiv:1906.08768 [hep-ph]
44. E. Kpatcha, I. Lara, D.E. López-Fogliani, C. Muñoz, N. Nagata, Explaining muon $g-2$ data in the $\mu\nu$SSM. Eur. Phys. J. C **81**(2), 154 (2021). https://doi.org/10.1140/epjc/s10052-021-08938-8. arXiv:1912.04163 [hep-ph]
45. P. Fayet, U-boson production in e+ e− annihilations, psi and Upsilon decays, and Light Dark Matter. Phys. Rev. D **75**, 115017 (2007). https://doi.org/10.1103/PhysRevD.75.115017. arXiv:hep-ph/0702176
46. M. Pospelov, Secluded U(1) below the weak scale. Phys. Rev. D **80**, 095002 (2009). https://doi.org/10.1103/PhysRevD.80.095002. arXiv:0811.1030 [hep-ph]

47. D. Tucker-Smith, I. Yavin, Muonic hydrogen and MeV forces. Phys. Rev. D **83**, 101702 (2011). https://doi.org/10.1103/PhysRevD.83.101702. arXiv:1011.4922 [hep-ph]
48. G. Mohlabeng, Revisiting the dark photon explanation of the muon anomalous magnetic moment. Phys. Rev. D **99**(11), 115001 (2019). https://doi.org/10.1103/PhysRevD.99.115001. arXiv:1902.05075 [hep-ph]
49. M. Fabbrichesi, E. Gabrielli, G. Lanfranchi, *in The Physics of the Dark Photon. SpringerBriefs in Physics* (Springer, Cham, 2020). https://doi.org/10.1007/978-3-030-62519-1. arXiv:2005.01515 [hep-ph]
50. P. Agrawal, Z. Chacko, C.B. Verhaaren, Leptophilic dark matter and the anomalous magnetic moment of the muon. JHEP **08**, 147 (2014). https://doi.org/10.1007/JHEP08(2014)147. arXiv:1402.7369 [hep-ph]
51. G. Bélanger, C. Delaunay, S. Westhoff, A dark matter relic from muon anomalies. Phys. Rev. D **92**, 055021 (2015). https://doi.org/10.1103/PhysRevD.92.055021. arXiv:1507.06660 [hep-ph]
52. K. Kowalska, E.M. Sessolo, Expectations for the muon g-2 in simplified models with dark matter. JHEP **09**, 112 (2017). https://doi.org/10.1007/JHEP09(2017)112. arXiv:1707.00753 [hep-ph]
53. L. Calibbi, R. Ziegler, J. Zupan, Minimal models for dark matter and the muon g-2 anomaly. JHEP **07**, 046 (2018). https://doi.org/10.1007/JHEP07(2018)046. arXiv:1804.00009 [hep-ph]
54. J. Kawamura, S. Okawa, Y. Omura, Current status and muon $g-2$ explanation of lepton portal dark matter. JHEP **08**, 042 (2020). https://doi.org/10.1007/JHEP08(2020)042. arXiv:2002.12534 [hep-ph]
55. S. Jana, P.K. Vishnu, W. Rodejohann, S. Saad, Dark matter assisted lepton anomalous magnetic moments and neutrino masses. Phys. Rev. D **102**(7), 075003 (2020). https://doi.org/10.1103/PhysRevD.102.075003. arXiv:2008.02377 [hep-ph]
56. K. Kaneta, H.S. Lee, S. Yun, Portal connecting dark photons and axions. Phys. Rev. Lett. **118**(10), 101802 (2017). https://doi.org/10.1103/PhysRevLett.118.101802. arXiv:1611.01466 [hep-ph]
57. S.M. Barr, E.M. Freire, A. Zee, A mechanism for large neutrino magnetic moments. Phys. Rev. Lett. **65**, 2626–2629 (1990). https://doi.org/10.1103/PhysRevLett.65.2626
58. K. Kannike, M. Raidal, D.M. Straub, A. Strumia, Anthropic solution to the magnetic muon anomaly: the charged see-saw. JHEP**02**, 106 (2012). https://doi.org/10.1007/JHEP02(2012)106. arXiv:1111.2551 [hep-ph] [Erratum: JHEP **10**, 136 (2012)]
59. R. Dermisek, A. Raval, Explanation of the muon g-2 anomaly with vectorlike leptons and its implications for Higgs decays. Phys. Rev. D **88**, 013017 (2013). https://doi.org/10.1103/PhysRevD.88.013017. arXiv:1305.3522 [hep-ph]
60. A. Crivellin, M. Hoferichter, P. Schmidt-Wellenburg, Combined explanations of $(g-2)_{\mu,e}$ and implications for a large muon EDM. Phys. Rev. D **98**(11), 113002 (2018). https://doi.org/10.1103/PhysRevD.98.113002. arXiv:1807.11484 [hep-ph]
61. P. de Niverville, H.S. Lee, M.S. Seo, Implications of the dark axion portal for the muon g−2, B factories, fixed target neutrino experiments, and beam dumps. Phys. Rev. D **98**(11), 115011 (2018). https://doi.org/10.1103/PhysRevD.98.115011. arXiv:1806.00757 [hep-ph]
62. G. Alonso-Álvarez, M.B. Gavela, P. Quilez, Axion couplings to electroweak gauge bosons. Eur. Phys. J. C **79**(3), 223 (2019). https://doi.org/10.1140/epjc/s10052-019-6732-5. arXiv:1811.05466 [hep-ph]
63. M. Bauer, M. Heiles, M. Neubert, A. Thamm, Axion-like particles at future colliders. Eur. Phys. J. C **79**(1), 74 (2019). https://doi.org/10.1140/epjc/s10052-019-6587-9. arXiv:1808.10323 [hep-ph]
64. K. Cheung, T.W. Kephart, W.Y. Keung, T.C. Yuan, Decay of Z boson into photon and unparticle. Phys. Lett. B **662**, 436–440 (2008). https://doi.org/10.1016/j.physletb.2008.03.037. arXiv:0801.1762 [hep-ph]
65. J. Jaeckel, M. Spannowsky, Probing MeV to 90 GeV axion-like particles with LEP and LHC. Phys. Lett. B **753**, 482–487 (2016). https://doi.org/10.1016/j.physletb.2015.12.037. arXiv:1509.00476 [hep-ph]
66. B. Batell, N. Lange, D. McKeen, M. Pospelov, A. Ritz, Muon anomalous magnetic moment through the leptonic Higgs portal. Phys. Rev. D **95**(7), 075003 (2017). https://doi.org/10.1103/PhysRevD.95.075003. arXiv:1606.04943 [hep-ph]
67. C.Y. Chen, M. Pospelov, Y.M. Zhong, Muon beam experiments to probe the dark sector. Phys. Rev. D **95**(11), 115005 (2017). https://doi.org/10.1103/PhysRevD.95.115005. arXiv:1701.07437 [hep-ph]
68. B. Batell, A. Freitas, A. Ismail, D. Mckeen, Flavor-specific scalar mediators. Phys. Rev. D **98**(5), 055026 (2018). https://doi.org/10.1103/PhysRevD.98.055026. arXiv:1712.10022 [hep-ph]
69. D. Croon, G. Elor, R.K. Leane, S.D. McDermott, Supernova muons: new constraints on Z' bosons, axions and ALPs. JHEP **01**, 107 (2021). https://doi.org/10.1007/JHEP01(2021)107. arXiv:2006.13942 [hep-ph]
70. J.P. Lees et al. (BaBar), Search for a muonic dark force at BABAR. Phys. Rev. D **94**(1), 011102 (2016). https://doi.org/10.1103/PhysRevD.94.011102. arXiv:1606.03501 [hep-ex]
71. A.M. Sirunyan et al. (CMS), Search for an $L_\mu - L_\tau$ gauge boson using Z→ 4μ events in proton–proton collisions at $\sqrt{s} =$ 13 TeV. Phys. Lett. B **792**, 345–368 (2019). https://doi.org/10.1016/j.physletb.2019.01.072. arXiv:1808.03684 [hep-ex]
72. A. Filippi, M. De Napoli, Searching in the dark: the hunt for the dark photon. Rev. Phys. **5**, 100042 (2020). https://doi.org/10.1016/j.revip.2020.100042. arXiv:2006.04640 [hep-ph]
73. J.P. Lees et al. (BaBar), Search for a dark photon in e^+e^- collisions at BaBar. Phys. Rev. Lett. **113**(20), 201801 (2014). https://doi.org/10.1103/PhysRevLett.113.201801. arXiv:1406.2980 [hep-xp]
74. J.R. Batley et al. (NA48/2), Search for the dark photon in π^0 decays. Phys. Lett. B **746**, 178–185 (2015). https://doi.org/10.1016/j.physletb.2015.04.068. arXiv:1504.00607 [hep-ex]
75. P. Ilten, Y. Soreq, J. Thaler, M. Williams, W. Xue, Proposed inclusive dark photon search at LHCb. Phys. Rev. Lett. **116**(25), 251803 (2016). https://doi.org/10.1103/PhysRevLett.116.251803. arXiv:1603.08926 [hep-ph]
76. R. Aaij et al. (LHCb), Search for $A' \to \mu^+\mu^-$ decays. Phys. Rev. Lett. **124**(4), 041801 (2020). https://doi.org/10.1103/PhysRevLett.124.041801. arXiv:1910.06926 [hep-ex]
77. A.M. Sirunyan et al. (CMS), Search for a narrow resonance lighter than 200 GeV decaying to a pair of muons in proton–proton collisions at $\sqrt{s}$ = TeV. Phys. Rev. Lett. **124**(13), 131802 (2020). https://doi.org/10.1103/PhysRevLett.124.131802. arXiv:1912.04776 [hep-ex]
78. D. Curtin, R. Essig, S. Gori, J. Shelton, Illuminating dark photons with high-energy colliders. JHEP **02**, 157 (2015). https://doi.org/10.1007/JHEP02(2015)157. arXiv:1412.0018 [hep-ph]